IEEE Access
Multidisciplinary ⋮ Rapid Review ⋮ Open Access Journal

Received June 17, 2021, accepted June 22, 2021, date of publication June 25, 2021, date of current version July 5, 2021.

Digital Object Identifier 10.1109/ACCESS.2021.3092337

Effective Automation of Distribution Systems With Joint Integration of DGs/ SVCs Considering Reconfiguration Capability by Jellyfish Search Algorithm

ABDULLAH M. SHAHEEN[1], ABDULLAH M. ElSAYED[2], AHMED R. GINIDI[1], EHAB E. ELATTAR[3], (Senior Member, IEEE), AND RAGAB A. El-SEHIEMY[4], (Senior Member, IEEE)

[1]Department of Electrical Engineering, Faculty of Engineering, Suez University, Suez 43518, Egypt
[2]Department of Electrical Engineering, Faculty of Engineering, Damietta University, Damietta 22052, Egypt
[3]Department of Electrical Engineering, College of Engineering, Taif University, Taif 21944, Saudi Arabia
[4]Department of Electrical Engineering, Faculty of Engineering, Kafrelsheikh University, Kafr El-Sheikh 33516, Egypt

Corresponding author: Ragab A. El-Sehiemy (elsehiemy@ieee.org)

This work was supported by the Taif University, Taif, Saudi Arabia, through the Taif University Researchers Supporting Project, under Grant TURSP-2020/86.

This work did not involve human subject or animals in its research.

ABSTRACT Power system operators and planners have progressively shown an interest in maximizing distribution automation technologies. The automated distribution systems (ADS) provide the capability of efficient and reliable control which require an optimal operation strategy to control the status of the line switches and also dispatch the controllable devices. Therefore, this paper introduces an efficient and robust technique based on Jellyfish Search Algorithm (JFSA) for optimal Volt/VAr coordination in ADSs based on joint distribution system reconfiguration (DSR), distributed generation units (DGs) integration and Distribution static VAr compensators (SVCs) operation. The suggested technique is used for the dynamic operation of ADS in order to minimize losses and reduce emissions when considering regular daily loading conditions. The 33-bus and 69-bus delivery DSs have been subjected to a variety of scenarios. These situations are mostly concerned with achieving optimum distribution system operation and control, as well as validating the proposed methodology. Despite the problem's complexity, the proposed technique based on JFSA is shown to be the best solution in all of the cases considered. Furthermore, a comparison of the proposed JFSA with other similar approaches demonstrates its usefulness as a method to be used in modern ADS control centers.

INDEX TERMS Distribution systems automation, static VAr compensators, reconfiguration, distributed generation units, jellyfish search algorithm.

I. INTRODUCTION

The traditional distribution systems face several operational and technical problems such as increased power losses, inadequate voltage regulation, unreliability, and service insecurity. The main reason of these problems is the speedy growth of power demand with restricted generation and transmission development [1]. Improving the performance of distribution systems aims to decrease the dissipated power significantly and to save a vast amount of dollars per year for the systems' owners. Besides, reliable and secure services of power can be accomplished to meet the customers' satisfaction [2].

To keep harmony with the continuous load growth and to ensure improved performance of distribution systems while reducing losses and increasing profits for the network, additional enhancement devices are commonly used. The usually used enhancement devices are the capacitor banks (CBs), distribution static VAr compensators (SVCs), and distributed generators (DGs), which are used either separately or in a combined matter [3]. In addition, controlling the topological

The associate editor coordinating the review of this manuscript and approving it for publication was Zhouyang Ren.

structure of the distribution systems can reduce power loss, enhance system voltage profile, improving system quality and reliability, which commonly known as distribution network reconfiguration (DSR). Automation of distribution systems is the backbone to achieve the advantages of these enhancement devices and maintain the desired distribution systems' performance.

The reconfiguration of the distribution systems is a procedure that permits the system to modify its topological structure during contingencies or under normal operating conditions [4], [5]. The DSR can be categorized into two types, which are static or dynamic reconfiguration. The former one considers all switches (manually or remotely controlled) and looks for an enhanced fixed topology at the planning stage. While the latter reconfiguration considers remotely controlled, switching only in the active network to eliminate grid congestions in real-time [6]. For the DSR functionality, many algorithms have been established in a separate manner to improve the performance of the distribution systems, such as the firefly algorithm and feasibility-preserving evolutionary optimization [7], [8].

Lately, the integration of DGs into distribution systems have key optimistic influences on distribution systems performance. This is owing to their capability to reduce the system power losses, enhance the voltage stability, increase the system reliability, and decrease the total pollution of the system based on DGs technology types [9]. The integration of the DGs in the distribution system is becoming an urgent necessity for several reasons, such as the dramatic increase in electrical load demand, the increased interest of environmental concerns that aim to decrease in system pollution, and the liberalization of the electrical power market [10]. Therefore, various DGs types are employed. These DGs can be classified based on their fuel energy into dispatchable and non-dispatchable units [11]. However, the inclusion of DGs in distribution systems raises the short circuit levels. For mitigating such situations, fault current limiters should be installed [12]. Owing to the expanded number of DGs, there have been current attempts towards exploiting their relatively high controllability to enhance the long-term voltage stability. This is one characteristic of the emergence of the so-called active distribution network.

Several techniques have been utilized to find the best allocations of the DGs such as particle swarm optimization, modified moth flame optimization techniques, and multi-objective opposition based chaotic differential evolution [3], [13] and [14]. Abo El-Ela et al. [15] utilized the equilibrium optimizer to allocate DGs of biomass type in the distribution systems. In this paper, minimizing the operating and maintenance costs of the DGs have been augmented with the power utilities' benefits and handled as single target. Added to that, sunflower optimizer has been performed with Monte-Carlo simulation to considering DGs of wind type [16]. In this paper, the wind uncertainties of the DGs were considered through while the CBs re-allocation were handled to minimize the distribution losses, but the environmental concerns were not considered. In [17], closed-form techniques (CFTs) have been utilized for the allocation of DGs and CBs for minimizing reactive power losses (RPL) in distribution systems. In [18], an adequate control technique was presented for reducing voltage deviations and voltage flickers in distribution networks including DGs of photovoltaic (PV) energy sources. This study utilized voltage sensitivities in regard to the injected real and reactive powers of PV-DGs which can be modelled in their single, double and triple diode equivalent circuit [19].

Employing the fixed CBs is considered as the old traditional improvement device for distribution systems. Consequently, many optimization schemes were presented to deal with the capacitors' optimal location problem. The economic gains of the fixed CBs differ mainly on capacitor numbers, sizes and appropriate selection policies to match load variations [20]. In [21], CFTs have been applied for allocating the CBs in distribution networks to maximize the reduction of costs. In this study, the costs of the installation and reactive power production of the CBS were handled while considering power losses as well. As a result of the continuous load variations during the daily hours and seasons variations, the fixed CBs may lose its economic and operation merits by increased power losses and operation instability. Numerous meta-heuristic algorithms have been applied to get the best places and sizes of the CBs on the distribution systems, such as hybrid loss sensitivity factor, salp swarm algorithm and sine cosine algorithm, fuzzy loss sensitivity factor with sine cosine algorithm, backtracking search technique [22]–[24]. Growing the demanding of reactive power will reduce the power factor, which reduces the capacity of the system. Beside the CBs devices, a thyristor-controlled reactor (TCR) is one of the advanced technologies that is used to compensate the reactive power in a smooth way. It is combined with other schemes such as CB [25]. This scheme represents the SVC, which is one of the most promising solutions that can decrease power losses, improve voltage profile, enhance power factor, and reduce harmonic distortion resulting from non-linear loads [26]. The SVCs can create balance in case of continuous changes in distribution systems since they are capable of adapt to the highly varying profile of the loads [27]. The optimal allocation of the SVC is addressed in the literature using different optimization algorithms such as artificial bee colony, cuckoo search algorithm, chemical reaction optimization, and grey wolf algorithm [28]–[30].

To maximize the gains from the above devices and techniques in enhancing the performance of distribution systems, two or more devices or strategies were concurrently employed. The DSR and CBs placement were concurrently presented in literature based on fuzzy binary gravitational search algorithm [30]; ant colony algorithm [31]. Also, DSR functionality and DGs allocation were concurrently presented using various methods, for example, dataset approach with marine predators algorithm [32]; coyote algorithm [33]; hybrid genetic algorithm, particle swarm optimization and blue whale optimization [34]. In addition, optimal placement

of CBs and DGs have been solved using particle swarm optimization [3], water cycle algorithm [35], enhanced grey wolf algorithm [36]. Added to that, an optimum approach was adopted to optimize the profit of the network operator by encouraging stability in the delivery of energy on the market by the management of real and reactive powers by scheduling the versatile loads and the associated photovoltaic DG modules [37]. However, the intelligent DSR function due to smart networks have been ignored whilst the system's reactive power supply necessitates further focus. For DG preparation combined with storage devices, an ant lion algorithm has been used in order to maximize the investment gains [38]. However, the planned DG positions were determined by the loss sensitivity index. It limits the searching space, and it is unsuitable for large-scale systems.

The enhancement devices, previously mentioned and others, cannot be employed properly as well DSR cannot pays off optimally in the non-ADS that sometimes have a reverse impact on the distribution system operation [39]. Automation of distribution systems is one of the most efficient structures for enhancing not only the efficiency of the systems but also increasing the reliability of the power service [40]. Accordingly, it can be say that, there are two main requirements for attaining the automation of distribution systems, which are controlling the automatic switches of distribution systems as well as controlling the connected dispatchable enhancement devices [39]. A complete automation of the distribution system where automatic switches exist in each branch section was considered. In the other hand, despite their wide penetration into modern power systems, DGs and SVCs have not been integrated in literature. In this article, dispatchable DGs with intentions control are regarded via consistent communications with the distribution system operator. Not just that, but SVCS, are involved and controlled as well. Secure communications and auto switches are the essential parts for extensive delivery automation [41], where the electrical grid and data transfer technologies should be built to manage an effective automation functionality for the distribution systems.

Due to the complexity and range of the control variables, it is difficult to implement concurrent control and ADS with SVCs, DGs, and DSR concurrently in previous literature searches. Furthermore, numerous literatures proposed the optimum operation of DSs based solely on peak demand, ignoring realistic load changes, which often conflicted with the functional operating requirements of the systems. The objective of this work is to fill this gap by developing the Jellyfish Search Algorithm (JFSA) for concurrent control of SVCs, DGs, and DSR. JFSA proposed in [42], is inspired from the jellyfish movements. They are arranged in three principles. Firstly, the jellyfish movements may be toward the ocean current or within its swarm. Secondly, when the food amount is fine, the jellyfishes are drawn to their places. Thirdly, the quantitative objective function demonstrates the amount of food. The JFSA is developed for handling the dynamic operation of ADS for losses minimization, and emissions reduction considering daily load variations. Different cases have been applied to the 33-bus and 69-bus distribution test systems. These cases aim, mainly, at achieving optimal operation and control of the distribution systems and to validate the proposed technique for the possibility of adopting it in distribution systems control centers. The main contributions can be organized as follows:

- Proposing a management procedure for SVCs and DGs with the aim of determining the optimum DSR.
- Developing the JFSA in order to solve the discussed concurrent control strategy for automating the DSs.
- The proposed ADS procedure is applied for two test systems, DSs under various load conditions.
- The simulation findings demonstrate the proposed JFSA's capabilities to achieve reasonable and substantial enhancements in the efficiency of the tested distribution systems in terms of power loss reduction, voltage profile enhancements, and pollution reduction.
- A comparative evaluation of the proposed JFSA is performed related to the algorithms in the literature.

The remainder of this work is structured as follows: The formulation of the problem is defined in Section 2. Section 3 describes the suggested optimization techniques as well as the implementation of the strategy method for solving the problem. Section 4 presents the numerical results as well as a discussion of the findings. Section 5 summarizes the paper's observations and results.

II. PROBLEM FORMULATION

The efforts of the distribution systems' planners and operators have not ceased to reach the best possible performance of the distribution networks and to overcome all operation and economic problems. The most serious of these problems is the poor power quality that results from the continuously increased load demand on the current passive traditional distribution systems, which suffers from obsolescence and the inability to control its various components. The economic side also represents an essential challenge in the economic operation of the electrical power systems in general and distribution systems in particular, as the electric utility incurs losses millions of dollars per day as a result of power losses only in distribution systems. Despite the developments that have occurred in the distribution systems in the last two decades from the use of fixed and switched capacitor banks and the use of renewable energy resources as a distributed generators and other enhancement devices that have led to change the shape and operation modes of distribution systems, poor planning of these devices may be worse in the operation of the distribution systems than before. As a result of the above, many researchers seek to provide efficient techniques for optimizing the distribution systems' structure, operation and control. Some of these solutions were to determine the optimal placement to connect these devices and their optimal sizes. Also, some researchers were directed on how to coordinate between some of these devices. As well, controlling the adjustable elements represent another goal. All these

were aimed at achieving a set of objectives that would satisfy consumers as well as electric utility. As well, enhancing voltage profile of distribution systems and efficient feeding make most of the modern loads run safely. In addition, the increased reliability of feeding systems increases consumers' satisfaction. Also, losses minimization and increasing the utilization of existing renewable resources lead to saving millions of dollars for electric utility and reducing harmful emissions.

The performance enhancement of distribution systems, for consumers and utility satisfaction, can be achieved with the following objectives functions [4]:

$$OF_1 = \min\left(\sum_{\mathrm{br}=1}^{\mathrm{N_{br}}} Ploss_{\mathrm{br}}\right) \tag{1}$$

$$OF_2 = \min\left(\mathrm{E_{Grid}}.P_{\mathrm{Grid}} + \mathrm{E_{DG}}.\sum_{\mathrm{i}=1}^{\mathrm{N_{DG}}} P_{DG-\mathrm{i}}\right) \tag{2}$$

where, $Ploss_{\mathrm{br}}$ and $\mathrm{N_{br}}$ are the real losses in each branch (br) and the number of DS segments, respectively. P_{Grid} and P_{DG} are the real power supplied from the grid and DGs, respectively. $\mathrm{E_{Grid}}$ and $\mathrm{E_{DG}}$ are the associated emissions per each hourly real power production (TonCo2/MWhr) from the grid and DGs, respectively. They are taken with 0.910 and 0.773 TonCo2/MWhr, respectively [43]. The weight sum approach, in conjunction with the normalization procedure, can be used to obtain the intended performance. [44], [45] :

$$Fitness = \omega_1 \frac{Ploss}{Ploss^{\max}} + \omega_2 \frac{Co_{2\ Emission}}{Emission^{\max}} \tag{3}$$

where, ω_1 *and* ω_2 are weight factors. *Ploss* and $Co_{2\ Emission}$ are total DS losses and the associated Carbon-dioxide emissions, respectively. $Ploss^{max}$ and $Emission^{\max}$ are their maximum values, respectively.

This target could be utilized to find the best operating values of SVCs, DGs, and DSR through varying load operation. DGs and SVCs are physically installed at specific points on the DS and cannot be modified. The sizes of the fixed capacitors and DGs are often set (non-dispatchable), resulting in unnecessary reverse power flow with loading conditions. The dispatchable operation of DGs and SVCs is needed for the efficient operation of distribution systems. Not just that, but it also necessitates DSR by the optimum adjustment in the status of the tie lines. As a result, the control variables are as follows:

$$\mathrm{CV} = \left\{ \begin{array}{c} \left(Q_{SVC-1}, Q_{SVC-2}, \ldots, Q_{SVC-\mathrm{N_{SVC}}}\right); \\ \left(P_{DG-1}, P_{DG-2}, \ldots, P_{DG-\mathrm{N_{DG}}}\right); \\ \left(T_{Ob-1}, T_{Ob-2}, \ldots, T_{Ob-\mathrm{N_{TOb}}}\right) \end{array} \right\} \tag{4}$$

where, Q_{SVC} and $\mathrm{N_{SVC}}$ are the generated reactive power from the SVC and their number, respectively. T_{Ob} and $\mathrm{N_{TOb}}$ are the opened tie branches and their number, respectively. $\mathrm{N_{DG}}$ are the number of DGs.

Each control variable must adhere to the operational constraints.

$$\mathrm{Q_{SVC}^{min}} \le Q_{SVC-k} \le \mathrm{Q_{SVC}^{max}}, \quad \mathrm{k} = 1, 2, \ldots, \mathrm{N_{SVC}} \tag{5}$$

$$\mathrm{P_{DG}^{min}} \le P_{DG-k} \le \mathrm{P_{DG}^{max}}, \quad \mathrm{k} = 1, 2, \ldots, \mathrm{N_{DG}} \tag{6}$$

$$1 \le T_{Ob-\mathrm{k}} \le \mathrm{T_{Ob-N_{TO}}}, \quad \mathrm{k} = 1, 2, \ldots, \mathrm{N_{TOb}} \tag{7}$$

where, $\mathrm{Q_{SVC}^{min}}$ and $\mathrm{Q_{SVC}^{max}}$ are the minimum and maximum absorbed/injected VAr outputs from SVCs, respectively. $\mathrm{P_{DG}^{min}}$ and $\mathrm{P_{DG}^{max}}$ are the minimum and maximum generated kW outputs from DGs, respectively.

The total produced power from active and reactive power sources should adhere to the constraints mentioned below.

$$\sum_{k=1}^{\mathrm{N_{DG}}} P_{DG-\mathrm{k}} \le \mathrm{PL_{DG}} \sum_{m=1}^{\mathrm{N_{bs}}} (\mathrm{PD_m}) \tag{8}$$

$$\sum_{\mathrm{k}=1}^{\mathrm{N_{SVC}}} Q_{SVC-k} \le \mathrm{QL_{SVC}} \sum_{m=1}^{\mathrm{N_{bs}}} (\mathrm{QD_m}) \tag{9}$$

where, $\mathrm{PL_{DG}}$ and $\mathrm{QL_{SVC}}$ are the permissible penetration limit of DGs and SVCs, respectively. $\mathrm{PD_m}$ and $\mathrm{QD_m}$ are the real and reactive power demands at bus m, respectively. $\mathrm{N_{bs}}$ is the number of DS buses.

The SVC reactive outputs may be injected/absorbed related to DS loading. In addition, powering all loads should be maintained at each loading as in Eqs. (10) and (11), as:

$$\left(P_{\mathrm{Grid}} + \sum_{\mathrm{i}=1}^{\mathrm{N_{DG}}} P_{DG-\mathrm{i}}\right)_{\mathrm{Lc}} > \sum_{m=1}^{\mathrm{N_{bs}}} (\mathrm{PD_m})_{\mathrm{Lc}}, \quad \mathrm{Lc} = 1, 2, \ldots, \mathrm{M_{Lc}} \tag{10}$$

$$\left(Q_{\mathrm{Grid}} + \sum_{\mathrm{k}=1}^{\mathrm{N_{SVC}}} Q_{SVC-k}\right)_{\mathrm{Lc}} > \sum_{m=1}^{\mathrm{N_{bs}}} (\mathrm{QD_m})_{\mathrm{Lc}}, \quad \mathrm{Lc} = 1, 2, \ldots, \mathrm{M_{Lc}} \tag{11}$$

where, Q_{Grid} is the supplied reactive power from the grid. $\mathrm{M_{LC}}$ is the number of loading levels.

Another constraint is to maintain the active and reactive balance at each load condition, according to Eqs. 12 and 13.

$$P_{\mathrm{Grid}} + \sum_{\mathrm{i}=1}^{\mathrm{N_{DG}}} P_{DG-\mathrm{i}} - \sum_{\mathrm{br}=1}^{\mathrm{N_{br}}} Ploss_{\mathrm{br}} = \sum_{m=1}^{\mathrm{N_{bs}}} \mathrm{PD_m} \tag{12}$$

$$Q_{\mathrm{Grid}} + \sum_{\mathrm{k}=1}^{\mathrm{N_{SVC}}} Q_{SVC-k} - \sum_{\mathrm{br}=1}^{\mathrm{N_{br}}} Qloss_{\mathrm{br}} = \sum_{m=1}^{\mathrm{N_{bs}}} \mathrm{QD_m} \tag{13}$$

where $Qloss_{\mathrm{br}}$ is the reactive power losses in each branch segment (br).

Finally, the optimized problem should maintain the distribution system buses voltages and branches current within the allowable limits as given in Eqs. 14 and 15.

$$\mathrm{V^{min}} \le V_{\mathrm{i}} \le \mathrm{V^{max}}, \quad \mathrm{i} = 1, 2, \ldots\ldots \mathrm{N_{bs}} \tag{14}$$

$$|I_{\mathrm{br}}| \le \mathrm{I_{br}^{max}}, \quad \mathrm{br} = 1, 2, \ldots, \mathrm{N_{br}} \tag{15}$$

where V_i, V_i^{max} and V_i^{min} are the value, maximum and minimum voltage magnitudes, respectively. I_{br} and I_{br}^{max} are the value and maximum limit of the current in each branch (br).

Furthermore, the radial topology of the network should be kept for operation. A branch-bus incidence matrix can be formed as given in Eq. (16). Based on the matrix formation which is a $N_{bs} \times N_{br}$, the network topology can be judged. The network topology is radial if their determinant is 1 or -1, and the network isn't radial if it is zero [46]:

$$A_{ij} = \begin{cases} 0, & \text{if line i is not connected to bus k} \\ -1, & \text{if the line i enter to bus k} \\ 1, & \text{if the line i exits from bus k} \end{cases} \quad (16)$$

III. JFSA FOR EFFECTIVE OPERATION OF ADS

In JFSA, the initial population of the jellyfishes is seeded in a diverse manner by chaotic logistic projection as:

$$X_i(t+1) = 4v_0(1 - X_i), \quad 0 \le v_0 \le 1 \quad (17)$$

where X_i represents the i^{th} jellyfish chaotic counterpart, and v_o a created random value of $v_0 \in (0, 1)$, $v_0 \notin \{0.0, 0.25, 0.75, 0.5, 1.0\}$.

The JFSA is modeled and governed by three rules as:

- the jellyfishes can travel towards to the ocean current or inside the swarm. The transition among such two modes is guided in this case via a timing control system (TCS).
- Second, whenever the food supply is adequate, the jellyfishes are attracted to their respective positions.
- Third, the objective value displays the quantity of food.

A time regulation variable *c(t)*, as defined by Eq. (18), is used for representing the TCS.

$$c(t) = \left| \left(1 - \frac{t}{Max_{iter}}\right) \times (2 \times rand(0, 1) - 1) \right| \quad (18)$$

where t is the current iteration while Max_{iter} is the whole iterations. The TCS ranges at random from zero to one. Based on 50 percent probability, the jellyfish can adopt the current of the ocean where its direction (trend) is estimated by using the mean of the jellyfishes (μ) and the best individual among them (X^*). As a result, the new jellyfish position is described as follows:

$$X_i(t+1) = R \times (X^* - 3 \times R \times \mu) + X_i(t) \quad (19)$$

where R is a number chosen at random from the range [0-1].

If the jellyfish doesn't follow the ocean current, it moves inside the swarm, which takes either the passive or active movement behaviors. In the passive type, the majority of jellyfishes move throughout their specific sites where each position is modified as follows:

$$X_i(t+1) = 0.1 \times R \times (U_b - L_b) + X_i(t) \quad (20)$$

where U_b and L_b represent, respectively, the higher and lower bounds of the design variables.

In the active type, when the volume of food at the position of the chosen jellyfish (j) surpasses their counterpart at (i), it begins to move towards the first as described in Eq. (21):

$$X_i(t+1) = \begin{cases} X_i(t) + R \times (X_j(t) - X_i(t)) & \text{if } f(X_i) \ge f(X_j) \\ X_i(t) + R \times (X_i(t) - X_j(t)) & \text{if } f(X_0) < f(X_j) \end{cases} \quad (21)$$

where f denotes the volume of food in terms of the objective valuation related to each jellyfish position.

The TCS is used to perform the selection criterion of passive and active types. In this regard, a number is randomly created from the range [0-1]. If this number is larger than the term $(1 - c(t))$, the jellyfish demonstrates the passive motion. Else, it demonstrates the active motion. As the TCS value declines from 1 to 0 through time, passive motion is preferred at first, and active motion is chosen as time passes.

A jellyfish can return to the reverse bound if it ventures past the bounded search field. This re-entry procedure is represented as follows:

$$\begin{cases} X'_{i,d} = (X_{i,d} - U_{b,d}) + L_b(d) & \text{if } X_{i,d} > U_{b,d} \\ X'_{i,d} = (X_{i,d} - L_{b,d}) + U_b(d) & \text{if } X_{i,d} < L_{b,d} \end{cases} \quad (22)$$

where, $X_{i,d}$ represents the i^{th} jellyfish position in d^{th} dimension to be modified after the boundaries are examined. Fig. 1 describes the JFSA steps.

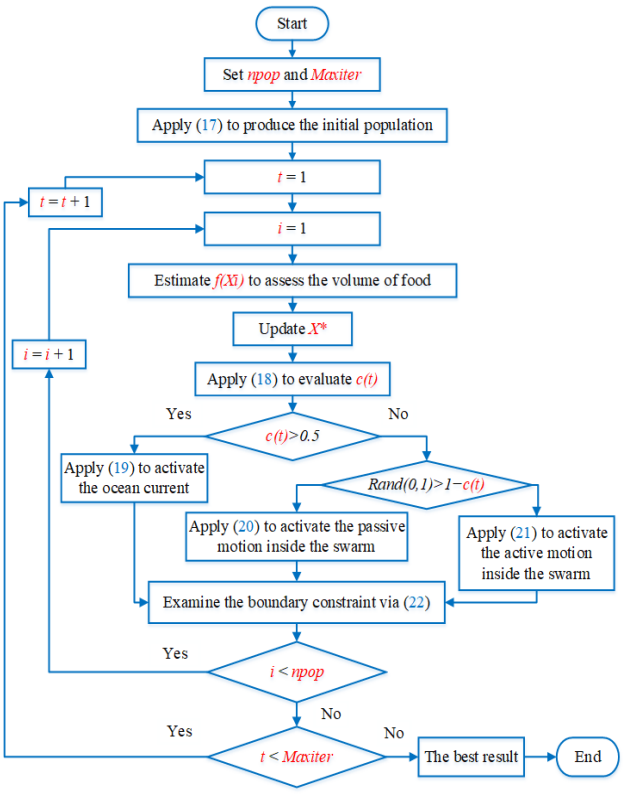

FIGURE 1. Main steps of JFSA.

In addition, Fig. 2 displays the JFSA development for handling the controlled operation of ADSs. As shown,

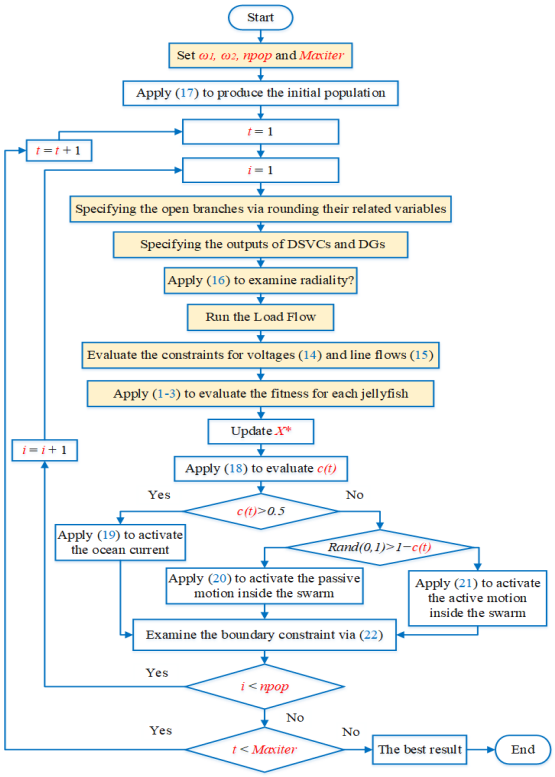

FIGURE 2. JFSA development for optimal operation of ADSs.

the control variables which are presented in (2) are considered. the regarding variables of the open tie branches are derived and rounded as they have a discrete nature. Also, the SVCs and DG outputs are specified. In addition, the configuration of the system is examined using Eq. (16) to assess if the ADS is radial. Then, the Load flow algorithm is executed via Newton Raphson tool and so the power losses in (1) and the carbon dioxide emissions in (2) are evaluated in order to estimate the fitness in (3). In each iteration, the inequality restrictions of the control variables (3)-(5) are preserved implicitly by testing their viability. Added to that, the inequality restrictions (6)-(11) are evaluated, and if there is a violation, the fitness takes infinity. Also, the Load Flow routine ensures Eqs. (12) and (13).

IV. SIMULATION RESULTS

A. TEST DSs

The JFSA is developed and evaluated on IEEE 33-bus and 69-bus distribution networks for optimal SVC, DGs and DSR coordination. The first network has 33 buses, 5 open links (L33- L37) and 32 sectionalizing links (L1-L32). In this system, the overall real and reactive demands are, respectively, 3.715 MW and 2.300 MVAr [47]. That system's initial power loss (initial topology without SVCs, DGs) is 202.69 kW whereas the minimum voltage is occurred at bus 18 with 0.9108 per unit (PU).

Secondly, a radial IEEE 69-bus DS of 12.66 kV, that consists of 69-bus with 68 sectionalizing links (L1-L68) and 5 open line segments (L69-L73) [48]. In this system, the overall real and reactive demands are, respectively, 3.8 MW and 2.69 MVAr. That system's initial power loss (initial topology without SVCs, DGs) is 224.95 kW whereas the minimum voltage is occurred with 0.909 (PU).

B. COMPARATIVE APPLICATIONS FOR OPTIMAL ALLOCATION OF DGs AND CBs

In this portion, a comparison of the JFSA with widely used techniques, that were previously reported in the literature, for improving the efficiency of the distribution system is investigated. This can be accomplished by combining the previously used optimum DGs and CBs allocations. As a result, the suggested JFSA is used to optimize the distribution of DGs and CBs when considering the maximum loading condition and the original configuration. The CBs are thought of in distinct sizes that are produced in 300 kVAr steps, while the highest rated capacity of any DG is 3 MW [49]. For the first system, the obtained DGs and CBs allocations based on the proposed JFSA are tabulated in Table 1 in comparison to manta ray foraging algorithm (MRFA) [47], [50], EGA [51], TSA [52], Improved TSA [52], WCA [35] and BFOA [59].

In these comparisons, no penetration limit in considered for installing new DGs in the DSs where the voltage limits are the same for all techniques. By means of the developed JFSA, as seen, buses 14, 24 and 30 are the selected buses to install DGs and CBs with 748, 1079 and 1056 kW and 300, 600 and 900 kVAr, respectively. Fig. 3 depicts the convergence rates of the implemented JFSA, which clearly explains its usefulness in optimizing the desirable response. Consequently, the power losses are significantly reduced from initially 202.69 to 12.572 kW representing a 93.89 percent decrease and demonstrating the highest reduction level of the other recorded algorithms. For the second system, the JFSA is used for optimum allocations of DGs and CBs considering the peak load state. Table 2 compares the related outputs to other methods of TSA, slime mould algorithm (SMA), crow search algorithm (CSO) and improved TSA [52]. CSO is effective recent algorithm that has been effectively applied to large scale optimization problems [53], [54]. Also, Fig. 4 depicts the enhancement of JFSA convergence properties for optimum CB and DG allocation. This contrast shows the efficacy of the suggested JFSA versus the others, where power losses are reduced from 224.95 kW to 4.68 kW with a 98.04% reduction.

Added to that, different separate runs are performed, and some statistical indicators are estimated such as the best, mean, median, worst, standard deviation and standard error are tabulated in Table 3. From this table, the developed JFSA has the ability to find minimum objectives with very small standard error of 0.0238 and 0.0138 for the 33-bus DS and the 69-bus DS, respectively.

For both DSs, Fig. 5 displays the histogram of the obtained losses by means of the developed JFSA for 30 separate runs. As shown, the developed JFSA declares high effectiveness since the majority of the losses are obtained in the least range.

TABLE 1. Optimal allocations of CBs and DGs at peak loading of the 33-bus system without DG penetration limits.

	Number of DGs/CBs	DGs Penetration (%)	Max./Min. voltage limits	Max./Min. voltage values	DGs bus location	DGs size (kW)	CBs bus location	CBs size (kVAr)	kW Losses
Initial	-	-	-	1/0.9105	-	-	-	-	202.69
BFOA [55]	3/3	42.98	NR	1/0.9783	17/ 18/ 33	542/ 160/ 895	18/ 33/ 30	163/ 338/ 541	41.41
WCA [35]	3/3	68.61	1.05/0.95	1/0.98	25/ 29/ 11	973/ 1040/ 536	23/ 30/ 14	465/ 565/ 535	24.68
TSA [52]	3/3	71.57	1.05/0.95	NR	24/ 30/ 12	766/ 917/ 976	30/ 11/ 24	1060/ 246/ 566	15.0
Improved TSA [52]	3/3	70.39	1.05/0.95	NR	13/ 25/ 30	788/ 742/ 1085	7/ 15/ 30	603/ 269/ 834	14.4
EGA [51]	3/3	76.094	1.05/0.95	1.003/0.9924	24/ 14/ 30	1094.96/ 767.74/ 964.22	25/ 14/ 30	388.75/ 334.77/ 1189.91	12.7
MRFA [49]	3/3	78.5	1.05/0.95	1.0016/0.992	13/ 24/ 30	803/ 1073/ 1040	14/ 24/ 30	300/ 600/ 900	12.572
Proposed JFSA	3/3	77.6	1.05/0.95	1.0015/0.992	14/ 24/ 30	748/ 1079/ 1056	14/ 24/ 30	300/ 600/ 900	**12.40**

NR indicates "Not Reported"

TABLE 2. Optimal allocations of CBs and DGs at peak loading of the 69-bus system without DG penetration limits.

	Number of DGs/CBs	Penetration (%)	Max/Min. voltage limits	Max./Min. voltage values	DGs bus location	DGs size (kW)	CBs bus location	CBs size (kVAr)	kW Losses
Initial	-	-	-	1/0. 9092	-	-	-	-	224.95
TSA [52]	3/3	65.97	1.05/0.95	NR	9/ 16/ 61	452/ 555/ 1500	21/ 53/ 61	299/ 605/ 1148	6.9
SMA [52]	3/3	58.78	1.05/0.95	NR	16/ 30/ 61	497/ 112/ 1625	2/ 13/ 61	708/ 623/ 1091	9.0053
CSO [52]	3/3	67.42	1.05/0.95	NR	17/ 61/ 67	535/ 1728/ 299	61/ 67/ 68	1367/ 311/ 323	7.5488
Improved TSA [52]	3/3	60.05	1.05/0.95	1.0024/0.9944	10/ 12/ 61	291/ 491/ 1500	9/ 23/ 61	288/ 292/ 1149	6.8012
Proposed JFSA	3/3	67.05	1.05/0.95	1.00438/0.994	11/ 18/ 61	495/ 379/ 1674	18/ 51/ 61	300/ 300/ 1200	**4.6826**

NR indicates "Not Reported"

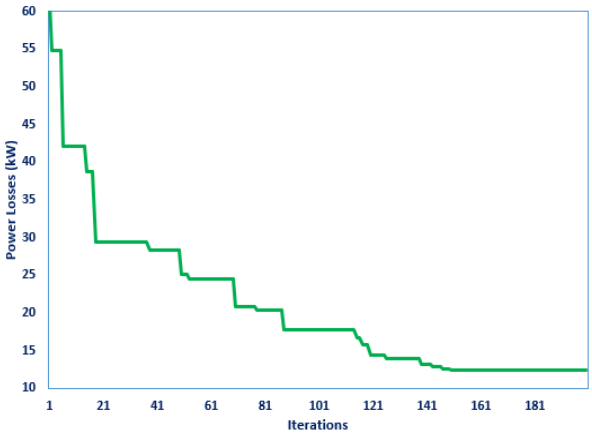

FIGURE 3. JFSA convergence rates for 33-bus system.

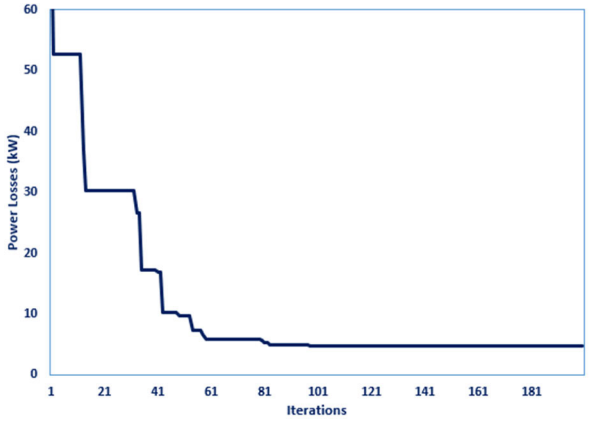

FIGURE 4. JFSA Convergence rates for 69-bus system.

TABLE 3. Statistical analysis of JFS for the 33 and 69-bus system.

	33 bus system	69-bus system
Best	12.4002	4.6826
mean	13.1092	5.4556
median	12.8021	5.4676
Worst	15.1889	6.2688
Standard deviation	0.7146	0.4151
Standard error	0.0238	0.0138

For the 33-bus DS, 19 runs with 63.33 % obtains losses in the least range from 12.4 to 13.2 kW. Also, 10 runs with 33.33 % obtains losses in the least range from 4.68 to 5.15 kW for the 69-bus DS.

C. MODIFICATIONS OF THE TEST DSs

As shown in the previous section, for the IEEE 30-bus DS, the developed JFSA proposes the optimal locations to install DGs and CBs at buses 14, 24 and 30. Based on that, this network has been adjusted such that 3 DGs with 1.1, 1, and 0.8 MW are installed, respectively at buses 30, 24, and 14, and a fixed capacitor is linked at bus 30 of 1.5 MVAr. Added to that, two SVCs are installed at buses 24 and 14, respectively with capacities of ± 1 MVAr. Fig. 6 depicts a graphical representation of all these modifications for the considered DS of IEEE 33-bus.

As shown in the previous section, for the IEEE 69-bus DS, the developed JFSA proposes optimal locations to install DGs at buses 11, 18 and 61 and CBs at buses 18, 51 and 61. Based on that, this network has been adjusted such that 3 DGs with 1.7, 0.5, and 0.5 MW are installed, respectively at buses 61, 18, and 11, and a fixed capacitor is linked at bus 61 of 1.5 MVAr. Added to that, two SVCs are installed at buses 51 and 18, respectively with capacities of ± 1 MVAr. Fig. 7 depicts a graphical representation of all these modifications for the considered DS of IEEE 69-bus. In this article, in Eq. (3), the Co_2 Emission^{max} is considered with 6 ton/hr.

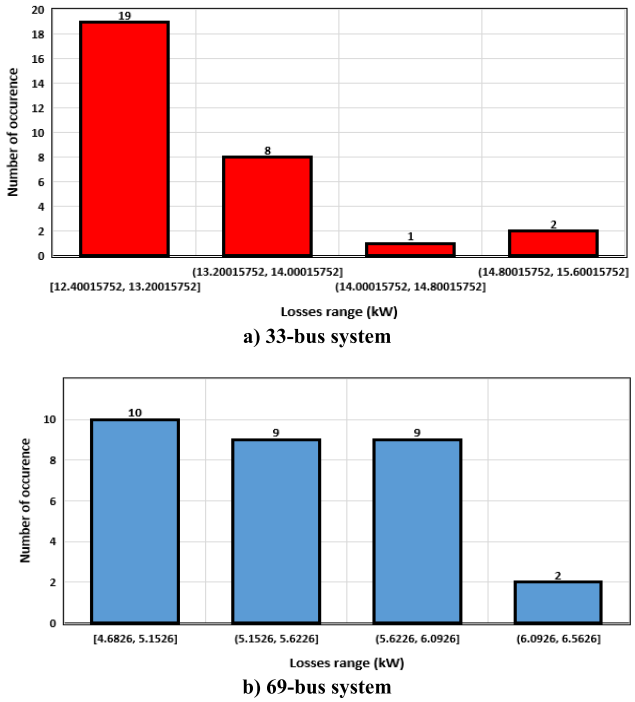

FIGURE 5. Histogram of the obtained power losses by means of JFSA for 33 and 69-bus DSs.

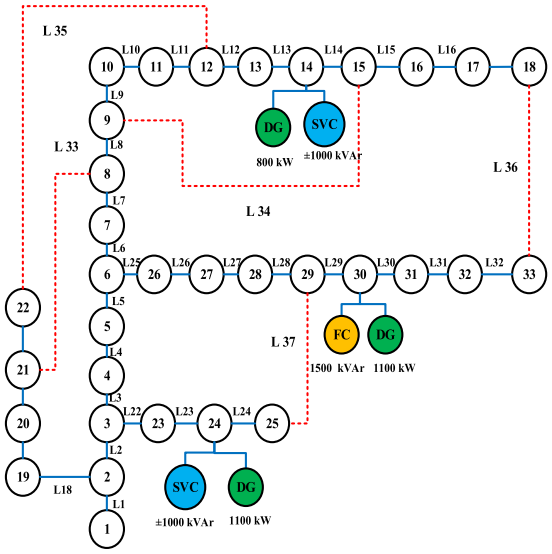

FIGURE 6. Adjusted IEEE 33-bus DS.

D. CASES STUDIED

As illustrated in Figs. 6 and 7, different devices such as DGs, SVCs, and CBs were used in the DSs under consideration. DSR features are also provided by sophisticated ADS. Therefore, the JFSA was commissioned to carry out two study cases compared with the main instance (***Case 0***). The executed cases demonstrate several operating strategies depending upon committed devices to be controlled:

Case 1: Optimal concurrent management of the injected/absorbed powers of SVCs and DGs, operating in dispatchable manner.

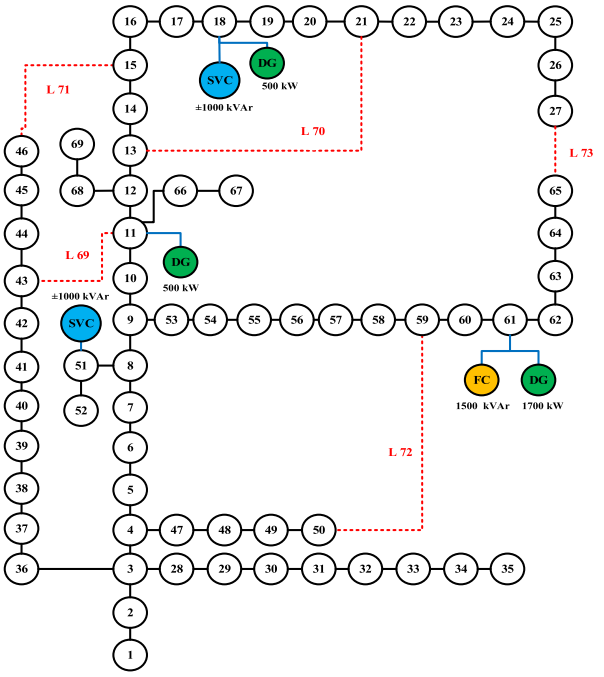

FIGURE 7. Adjusted IEEE 69-bus DS.

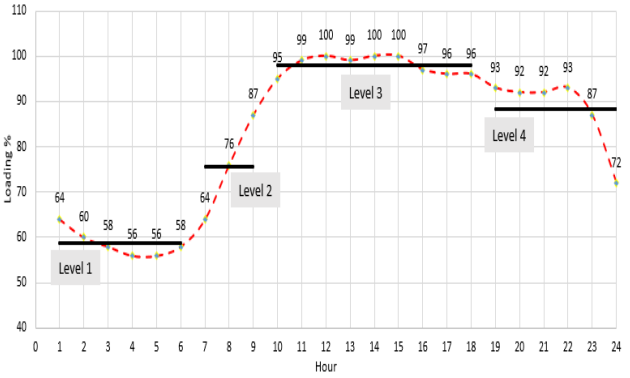

FIGURE 8. Loading % per hour.

TABLE 4. Results of *Case 0* at each load level of the 33-bus system.

Loading Level	One	Two	Three	Four
Total Load (MW)	2.1792	2.8108	3.6407	3.2766
Emissions ($tonCo_2/h$)	1.6939	2.235163	2.960072	2.640096
Losses (kWh)	133.8576	97.10242	63.77455	76.22303
Objective	1.174701	1.019877	0.918509	0.94817
Min-V (bus)	0.9979 (22)	0.9965 (22)	0.9946 (22)	0.9955 (22)
Max-V (bus)	1.0704 (14)	1.0571 (14)	1.0391 (14)	1.047(14)
Emissions /day = 59.3501 $tonCo_2$; Energy loss/day = 2125.762 kWh				

Case 2: Optimal concurrent management is introduced of dispatchable injected/absorbed powers of SVCs and DGs coordinated with tie switches of DSR.

In practice, the DS loadings are always changing. As a result, the operational control of the associated DGs, SVCs and DSR scheduling are being properly automated to minimize power losses and reduce emissions while considering load profile changes. The load profile variation in the

TABLE 5. Results of *Case 1* at each load level of the 33-bus system.

Items		Loading Level			
		One	Two	Three	Four
Active power outputs of the DGs (kW)	DG1	408	523	671	605
	DG2	397	495	622	571
	DG3	502	668	891	789
Reactive power outputs of SVCs (kVAr)	SVC1	-49	61	205	142
	SVC2	95	222	399	321
Penetration Ratio		59.97 %	59.983 %	59.988 %	59.97 %
Emissions (tonCo_2/h)		1.830282387	2.348863255	3.033983725	2.732999835
Losses (kWh)		28.84845868	24.22578565	22.14804938	22.49619252
Objective		0.497370122	0.552982447	0.653317617	0.605474589
Min-V (bus)		0.989913 (18)	0.988715 (18)	0.986946 (18)	0.987648 (18)
Max-V (bus)		1.012902 (30)	1.008787 (30)	1.003388 (30)	1.0105638 (30)
Emissions per day = 61.72155 tonCo_2; Energy losses per day = 580.07 kWh					

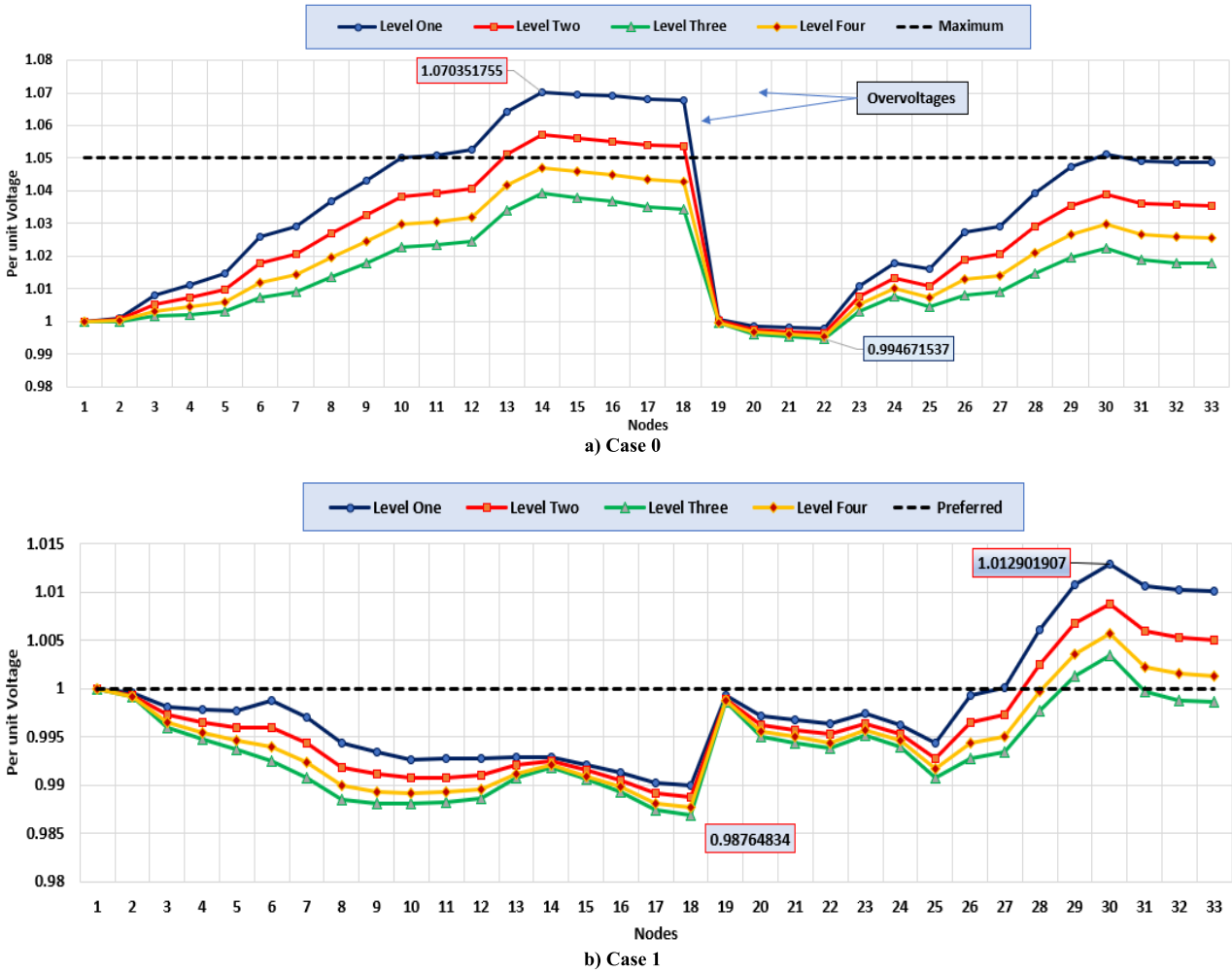

FIGURE 9. Voltage profile for *Case 0* and *Case 1* at each load level of the 33-bus system.

day is seen in Fig. 8 which is considered. From Fig. 8, there are four load levels per the day [56].

E. SIMULATION RESULTS OF THE 33-BUS DS

Analysis of Case 0: Case 0 indicates the DS initial case without dispatching on DGs and SVCs considering initial topology. DGs and SVCs are injecting their highest output without control. Throughout this case, the power flow is executed for each of the defined loading levels. Table 4 summarizes the acquired results. According to the data in such table, the power losses are 133.8576, 97.10242, 63.77455 and 76.22303 kW for the levels 1-4, respectively. Such losses account for 6.14, 3.49, 1.81, and 2.36 percent of the corresponding power demand, respectively. As shown, in the lowest loading, the maximum percent in power losses is existed and the highest voltage of 1.0704 PU is displayed.

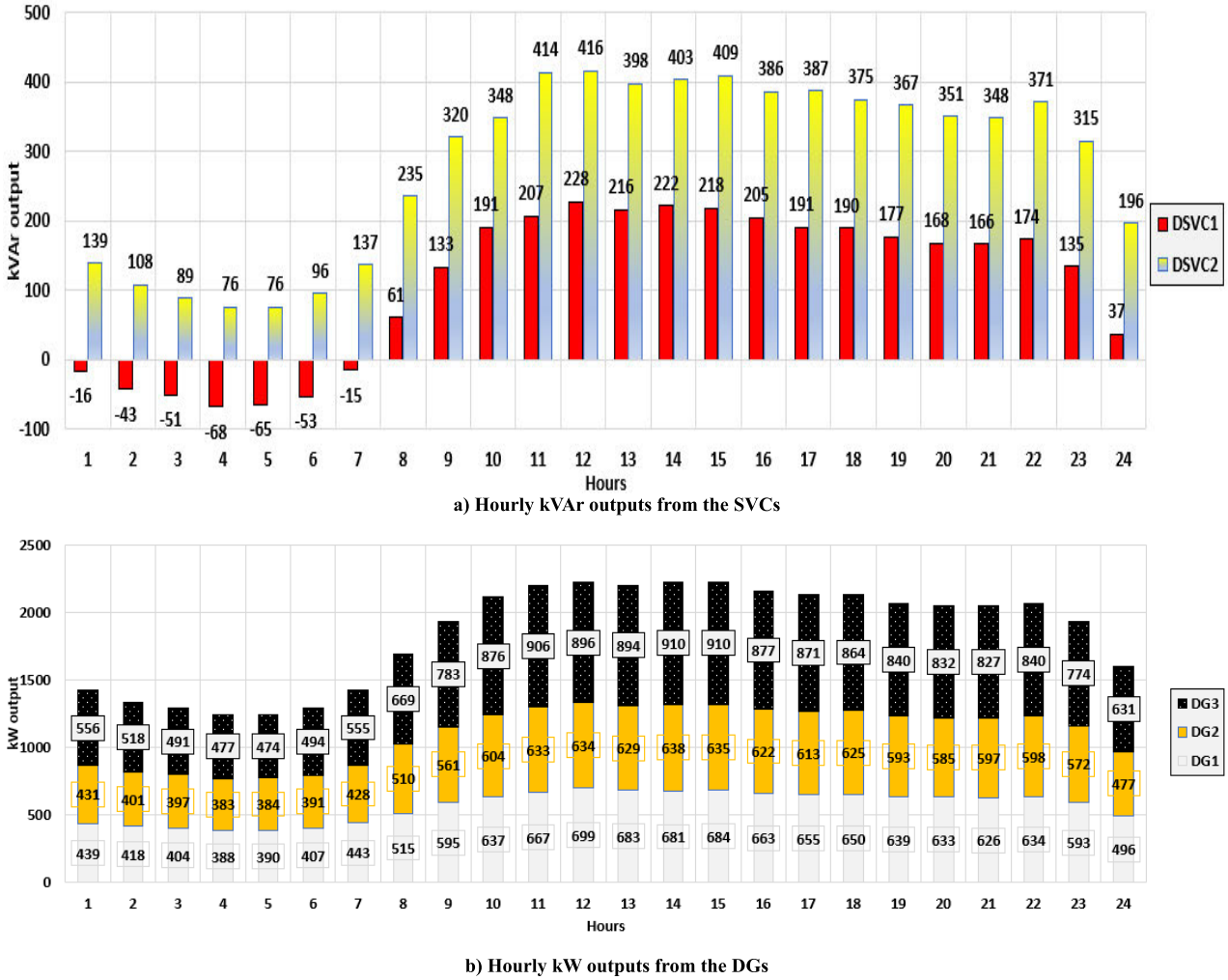

FIGURE 10. Optimal coordination of the DGs and SVCs at each hour of the 33-bus system.

For levels 1 and 2, the highest voltage values are, respectively, 1.0704 and 1.057 p.u which surpass the specified threshold of 1.05 p.u., although the comparable highest voltages for the remaining instances are not much further off. As a result, growing losses percentage and surpassing voltages highlight the need of optimal regulation of real and reactive supplies.

1) OPTIMAL CONTROL OF SVCs AND DGs (CASE 1)

In Case 1, Depending on the JFSA, the real and reactive power injections from DGs and SVCs are optimally managed, and the simulated results are given in Table 5. The achieved findings demonstrate that dissipated energy per the day is decreased from 2125.76 to 580.07 kWh with a significant decrease of 72.71 percent, whereas the pollutants value remains constant at 61.72 tons of CO2 per day. Furthermore, at the minimum loading, the excess voltages are rectified from 1.07 p.u. to 1.0129 p.u. That enhancement is obtained by running the first SVC in its −49 kVAr absorption condition. Consequently, with the next loading, the excess voltage values are rectified from 1.057 PU to 1.0087 PU. Additionally, the DGs and SVCs are also under concurrent management via the application of the proposed JFSA (*Case 1*). Also, Fig. 9 describes the significant improvement in DS voltage quality where it is highly enhanced for the DS buses towards being near to the desired value (1 p.u.) among all load levels in *Case 0*. From Table 5, losses (kWh) decrease by the increase of load level, however it is usual to be opposite.

The main reason for that is the existence of a fixed capacitor (FC) at bus 30 as described initially in Fig. 6. Thus, the decrease of the losses with increase in demand is matched with Table 4 as well. The FC injects nominally 1500 kVAr at the installed bus at all loading levels As the injected reactive power is directly proportional to the square of bus voltage [1], the injected kVAr is increased with the decrease of load. Also, the JFSA optimizes the SVCs reactive power outputs to enhance the voltage profile and treat the negative impacts of FC at light loading. As shown, the maximum voltage at loading level one occurred at bus 14 (1.0704 p.u.) as in Table 4. It is greatly enhanced after JFSA application and the maximum voltage at loading level one becomes at bus 30 of 1.0129 (Table 5). Also, the penetration ratio for all loading conditions equals 59.97%, 59.98%, 59.99% and

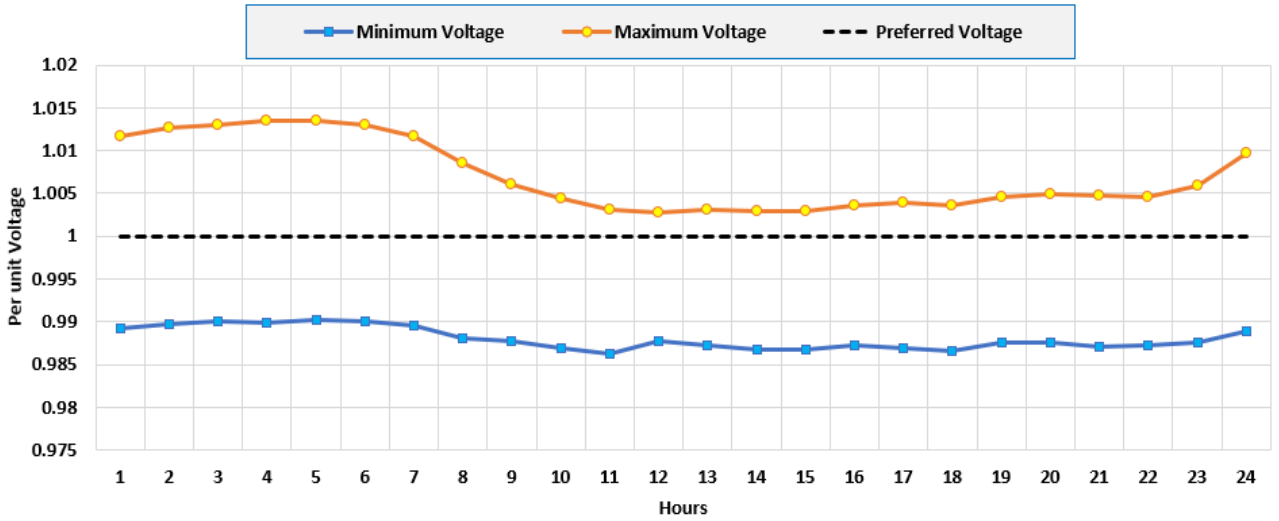

FIGURE 11. Minimum and maximum voltages based on the optimal coordination of the DGs and SVCs at each hour of the 33-bus system.

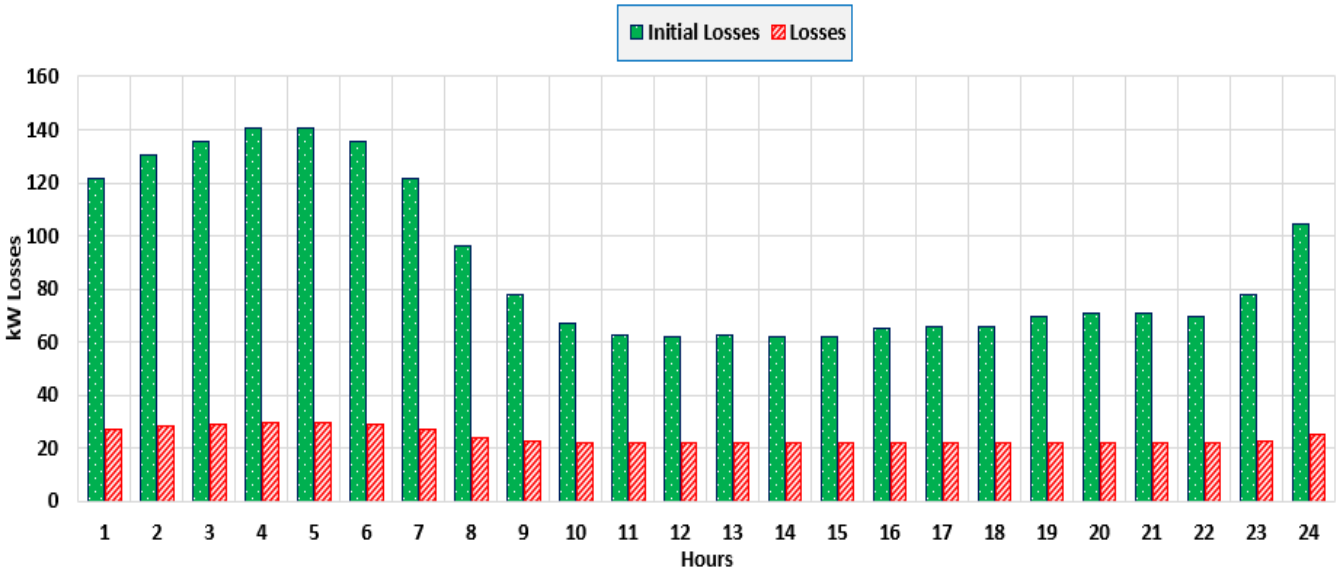

FIGURE 12. The hourly power losses based on the optimal coordination of the DGs and SVCs at each hour of the 33-bus.

59.97% for loading levels 1-4, respectively. It is noted that the penetration ratio is preserved and kept below the target level of 60%. Considering hourly loading changes, the proposed JFSA is used to efficiently manage the power injections from DGs and SVCs. Fig. 10 displays their hourly kW and kVAr outputs, respectively. The main particularity in using the SVC based FACTS devices compared to conventional compensators is related to their flexible control to exchange the reactive network with the network. Therefore, the outputs of the SVCs are approximately to the nearest integer since it is illustrated in kVar unit.

As shown, SVCs provides significant ability in managing the voltages since the first SVC is absorbing the surplus reactive power of the DS where the proposed JFSA optimizes it in negative value. The next SVC decreases its kVAr reactive output to accommodate the lower loading conditions during the first 7 hours. Consequently, when the loading grows within following hours, SVCs significantly raise their output kVar injections.

Fig. 11 demonstrates the improvement of the system's voltages with daily loading changes as the operating range of the buses voltage values at each hour are between 0.985 and 1.025 p.u. Furthermore, employing the JFSA to coordinates the DGs with the SVC injections considerably reduce the DS losses across the line segments, as shown in Fig. 12. When opposed to Case 0, this graph indicates a significant decrease in hourly DS losses.

2) OPTIMAL CONTROL OF SVCs AND DGs INVOLVING DSR (CASE 2)

In Case 2, the DSR is effectively integrated concurrently with optimum management of DGs and SVCs via the

TABLE 6. Results of *Case 2* at each load level of the 33-bus system.

Items		Loading Level			
		One	Two	Three	Four
Active power outputs of the DGs (kW)	DG1	364	450	582	481
	DG2	441	490	551	598
	DG3	502	745	1050	886
outputs of SVCs (kVAr)	SVC1	-56	39	290	276
	SVC2	-296	-160	7	-79
Open Switches		7, 8, 11, 12, 33	7, 8, 11, 12, 23	7, 8, 9, 17, 25	7, 11, 9, 17, 23
Penetration Ratio		59.975 %	59.948 %	59.961 %	59.97 %
Emissions ($tonCo_2/h$)		1.814559	2.338779	3.029357	2.726031
Losses (kWh)		11.5696749	12.99400151	16.91354023	14.83771116
Objective		0.379557615	0.476423232	0.617649822	0.553256511
Min-V (bus)		0.989967 (11)	0.987577 (11)	0.98713 (8)	0.988072 (8)
Max-V (bus)		1.000055 (30)	1 (1)	1 (1)	1 (1)
Emissions per day = 61.515 $tonCo_2$; Energy losses per day = 346.881 kWh					

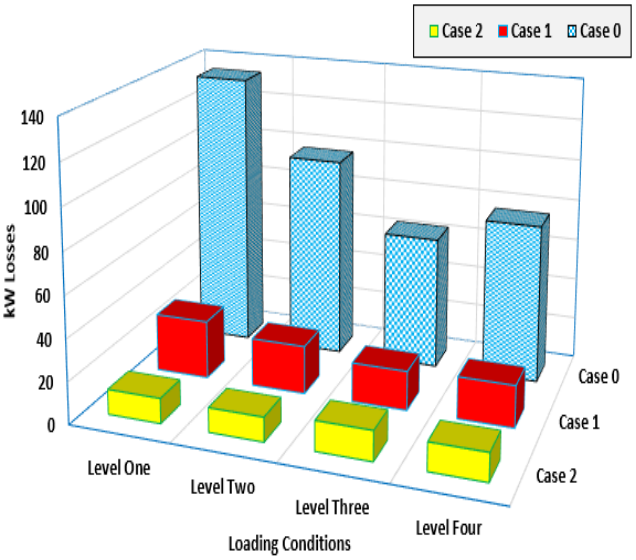

FIGURE 13. kWh Losses at each load level of the 33-bus system.

suggested JFSA. Table 6 summarizes the simulated findings. As indicated, a greater decrease in the dissipated energy per day is obtained, is becoming 346.881 comparing to 2125.762 and 580.07 kWh for *Cases 0* and *1*, respectively. Furthermore, as shown in Fig. 13, DS losses are minimized throughout the loading conditions in comparison to *Cases 0* and *1*. Associated with the proposed JFSA results in Table 6, the 2nd SVC runs at −296.0, −160.0, 7.0, and −79.0 kVAr for the four loading conditions, respectively. Such absorbed reactive energies enhance the DS voltages quality, whereby highest voltage values are about one p.u.

Also, the constraint of the penetration ratio is preserved for all loading conditions. Its value is 59.975, 59.948, 59.961 and 59.97 % % for loading levels 1-4, respectively, which is always less than the considered percentage of 60%.

F. SIMULATION RESULTS OF THE 69-BUS TEST SYSTEM

In *Case 0*, the power flow is executed to every specified load condition and the outcomes are shown in Table 7.

TABLE 7. Results of *Case 0* at each load level of the 69-bus system.

Loading Level	One	Two	Three	Four
Total Load (MW)	2.2299	2.8761	3.7254	3.3528
Emissions tonCo2/h)	1.759728	2.315153	3.059963	2.731062
Losses (kWh)	110.3551	74.47639	43.71768	54.82411
Objective	1.028989	0.882368	0.801445	0.820671
Min-V (bus)	0.9968 (50)	0.9958 (50)	0.9944 (50)	0.995 (50)
Max-V (bus)	1.0431 (61)	1.02977 (61)	1.0182 (61)	1.0221 (61)
Emissions per day = 61.4298 $tonCo_2$; Energy losses per day = 1607.9433 kWh				

According to above table, the DS losses for every load condition are 110.350, 74.480, 43.70, and 54.820 kW. Such power losses account for 5.17 percent, 2.84 percent, 1.39 percent, and 1.61 percent of the overall load, respectively.

In *Case 1*, the JFSA optimizes the DGs and SVCs outputs with loading changes. Various loading levels are evaluated then the daily loading changes per day is used to model the dynamic operations of a completely ADSs. Table 8 reports the findings for the four loading conditions. The daily wasted energy is decreased from 1607.940 to 308.473 kWh with 80.81% savings while the daily emissions equal 62 tonCo2.

Additionally, employing the suggested JFSA (Case 1) to regulate the SVCs and DGs concurrently enhances the DS buses voltage at all load conditions as depicted in Fig. 14. Highest voltage values at bus 61 are revealed to be 1.005, 1.0065, 1.0044, and 1.005 for all loading levels, whereas highest voltage values at *Case 0* are 1.043, 1.0297, 1.018, and 1.022. That enhancement is obtained by the first SVC device in absorbing operation at levels 1, 2 and 4, with -532.0, −289.0, and −97.0 kVAr. Considering the described earlier hourly loading changes, the suggested JFSA is used for optimal regulation of the injected powers from DGs and SVC, accordingly.

Fig. 15 shows the optimal coordination of the DGs and SVCs for each hour of the 69-bus system. In this figure, the capability of the SVCs is very high in controlling the voltage where the first SVC operates with negative values in absorbing the excessive kVAr from the system in the first six hours. After that, both SVCs increase their outputs with increasing the loadings in the next hours. Fig. 16 explains the high capabilities in the system voltages improvement with the daily load variations since the maximum and minimum

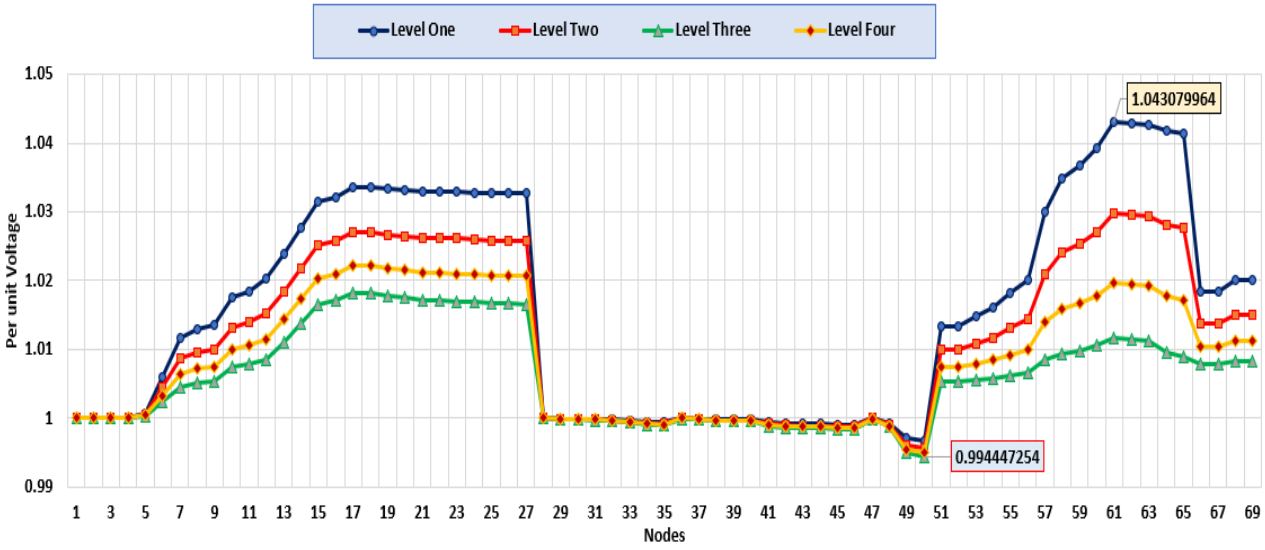

a) Case 0

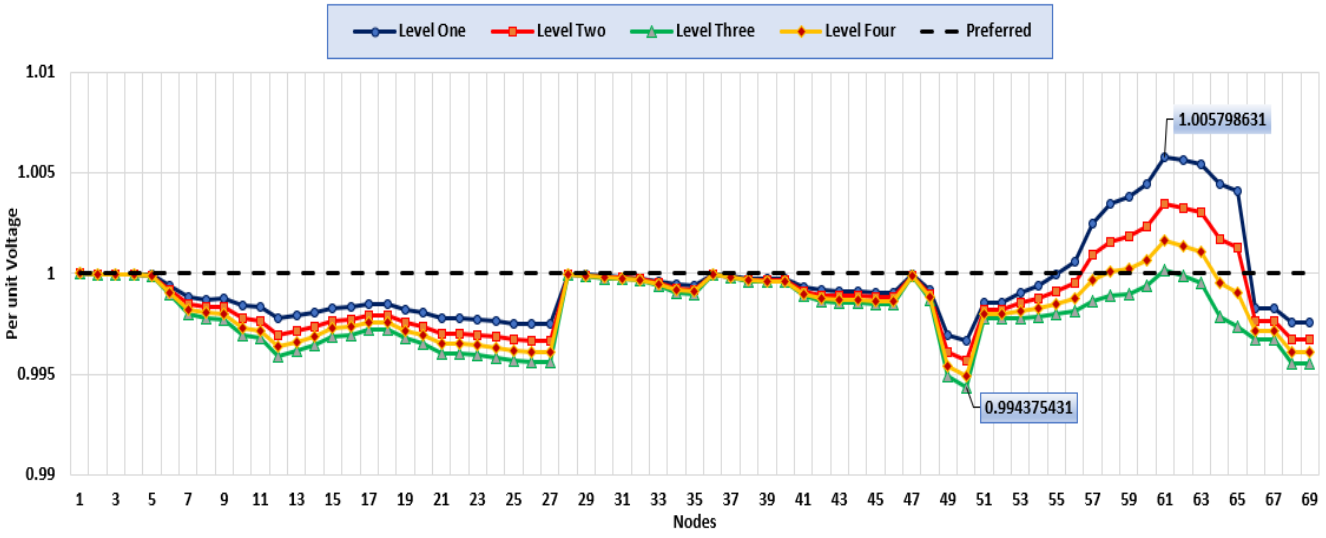

b) Case 1

FIGURE 14. Voltage profile for *Case 0* and *Case 1* at each load level of the 69-bus system.

TABLE 8. Results of *Case 1* at each load level of the 69-bus system.

Items		Loading Level			
		One	Two	Three	Four
Active power outputs of the DGs (kW)	DG1	207	243	294	271
	DG2	222	285	371	335
	DG3	908	1197	1570	1405
Reactive power outputs of SVCs (kVAr)	SVC1	162	224	298	263
	SVC2	-532	-289	43	-97
Penetration Ratio		59.979 %	59.998 %	60 %	60 %
Emissions ($tonCo_2/h$)		1.865421	2.393665	3.091653	2.78496
Losses (kWh)		21.30219	13.96701	8.536412	10.32477
Objective		0.452918	0.492058	0.572185	0.532992
Min-V (bus)		0.9966 (50)	0.9956 (50)	0.9944 (50)	0.9949 (50)
Max-V (bus)		1.005003 (61)	1.006569 (61)	1.00438 (61)	1.005056 (61)
Emissions per day = 62.8907 $tonCo_2$; Energy losses per day = 308.473 kWh					

voltages at any hour are within the range of 0.994 and 1.007 p.u. Furthermore, the coordination between the DGs outputs with the SVCs outputs are using the JFSA is achieved ideally and can decreases the power losses through the

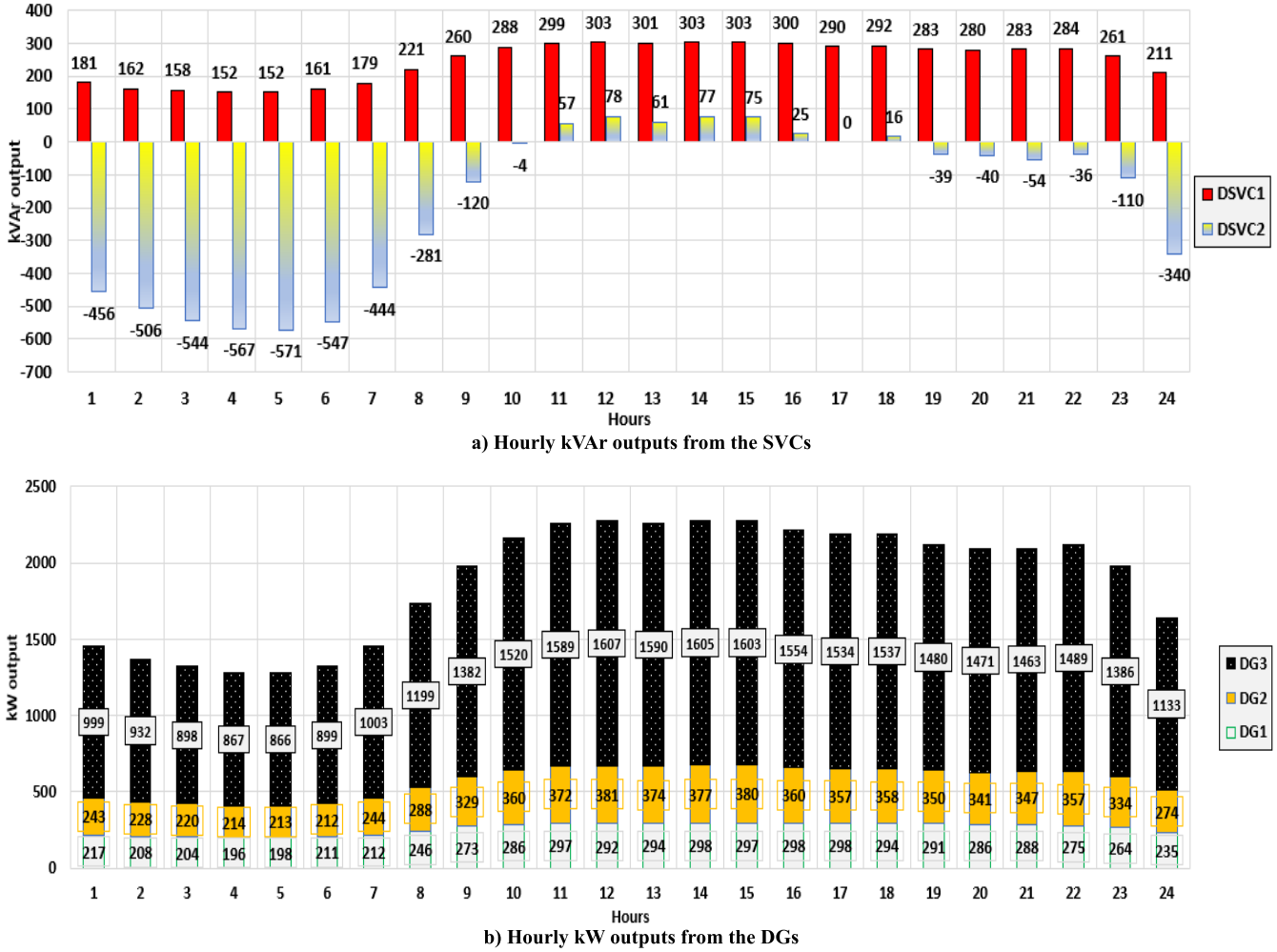

FIGURE 15. Optimal coordination of the DGs and SVCs for each hour of the 69-bus system.

TABLE 9. Results of *Case 2* at each load level of the 69-bus system.

Items		Loading Level			
		One	Two	Three	Four
Active power outputs of the DGs (kW)	DG1	295	327	276	272
	DG2	246	320	296	232
	DG3	796	1044	1663	1492
Reactive power outputs of SVCs (kVAr)	SVC1	36	67	305	259
	SVC2	53	285	184	123
Open Switches		10, 14, 15, 40, 53	10, 12, 13, 15, 52	10, 13, 15, 22, 54	10, 14, 15, 21, 52
Penetration Ratio		59.97 %	59.98 %	59.97 %	59.98 %
Emissions ($tonCo_2/h$)		1.855467	2.393969	3.090026	2.784349
Losses (kWh)		10.36394	9.182556	6.748813	7.394494
Objective		0.378337	0.460212	0.559996	0.513355
Min-V (bus)		0.999057 (10)	0.99544 (69)	0.994265 (69)	0.994378 (69)
Max-V (bus)		1.004803 (61)	1.00254 (61)	1.00044 (61)	1.002727 (61)
Emissions per day = 62.8275 $tonCo_2$; Energy losses per day = 194.821 kWh					

distribution lines, as illustrated in Fig. 17. It depicts the great reduction in the losses for each hour compared to *Case 0*.

In case 2, the proposed JFSA is applied for optimal DSR concurrently with controlling the SVCs and DGs outputs. The simulation results are recorded in Table 9. Fig. 18 displays the power losses for each load level compared to *Case 0* and *Case 1*. From both cases, more reduction is acquired in the daily dissipated energy, which becomes 194.821 kWh in *Case 2* compared to 1607.94 kWh in *Case 0* and 308.473 kWh in *Case 1*.

Additionally, the constraint of the penetration ratio is preserved for all loading conditions. Its value is 59.97, 59.98, 59.97 and 59.98 % % for loading levels 1-4, respectively, which is always less than the considered percentage of 60%

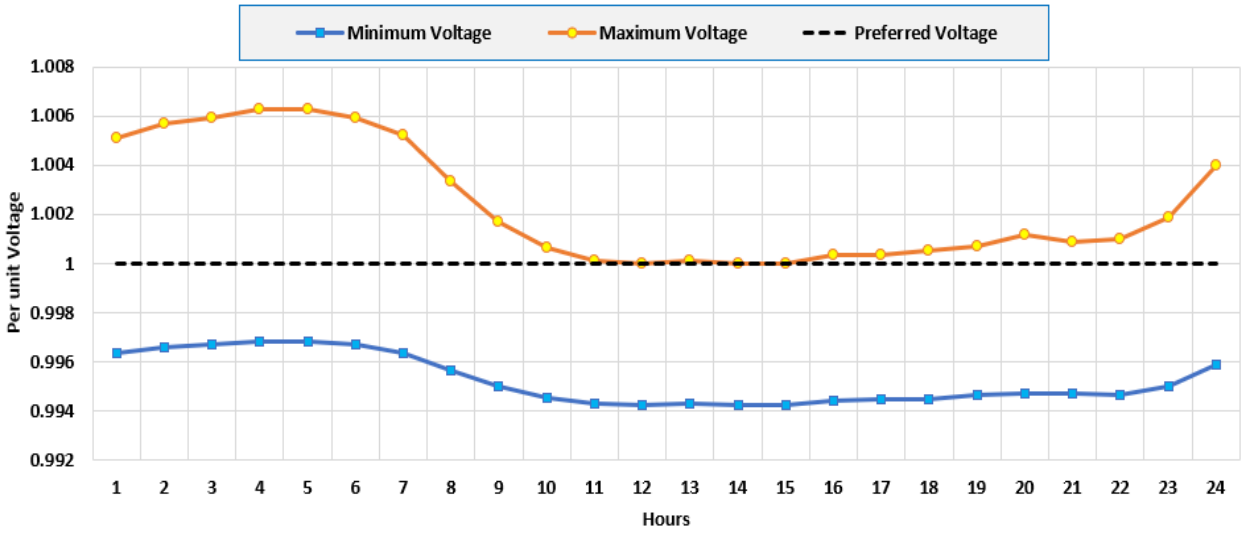

FIGURE 16. Minimum and maximum voltages based on the optimal coordination of the DGs and SVCs for each hour of the 69-bus system.

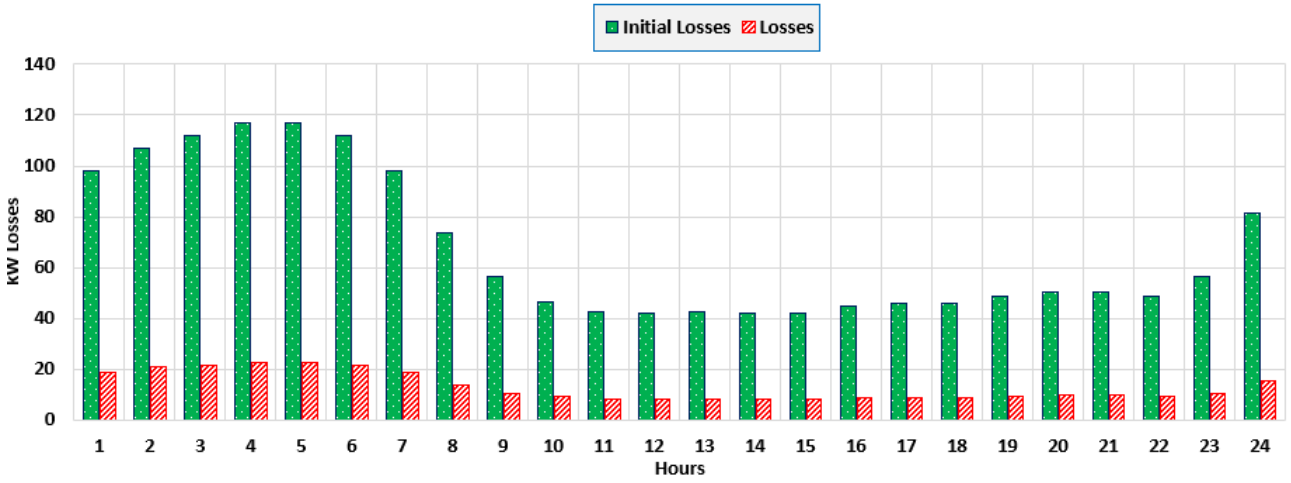

FIGURE 17. Power losses based on the optimal coordination of the DGs and SVCs for each hour of the 69-bus system.

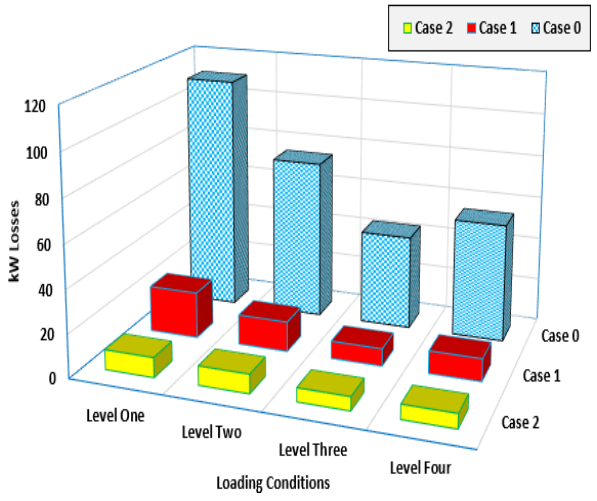

FIGURE 18. kWh Losses for Cases 0, 1, and 2 at each load level of the 69-bus system.

V. CONCLUSION

This paper introduces a new recent JFSA for optimal and effective operational control in the ADSs with optimally dispatching the connected dispatchable enhancement devices such as SVCs and DGs, with DSR activity all at the same time. The suggested technique is used for the dynamic operation of ADSs in order to minimize losses and reduce emissions when considering regular load variations. The 33-bus and 69-bus DSs have been subjected to a variety of scenarios. The proposed procedure is successfully applied to control the SVCs and DGs. It effectively controls the mode of operation of the SVCs in either injected or absorbed mode to enhance the DS voltage profile under the hourly load variations. The JFSA is successed in reducing the dissipated energy, in some cases, to 85.3% of the corresponding value of initial non-automated and not-controlled systems. This, in addition to keeping the emissions tonCo2 per day at minimum values. Not only that, but great voltage enhancement can also be

achieved using the proposed JFSA where the voltages at all system buses is closely to the preferred flat voltage 1 p.u. Also, comparative evaluation of the proposed JFSA with other related techniques of MRFA, EGA, TSA, WCA, SMA, BFOA and CSO demonstrate the effectiveness of the proposed JFSA to be effective tool to be utilized in control centers of distribution systems. Moreover, the histogram of the obtained power losses by means of the developed JFSA declares its high efficiency.

ACKNOWLEDGMENT

The authors would like to acknowledge the financial support received from Taif University Researchers Supporting Project Number (TURSP-2020/86), Taif University, Taif, Saudi Arabia.

REFERENCES

[1] A. M. Shaheen and R. A. El-Sehiemy, "A multiobjective salp optimization algorithm for techno-economic-based performance enhancement of distribution networks," *IEEE Syst. J.*, vol. 15, no. 1, pp. 1458–1466, Mar. 2021, doi: 10.1109/JSYST.2020.2964743.

[2] A. M. Elsayed, M. M. Hegab, and S. M. Farrag, "Smart residential load management technique for distribution systems' performance enhancement and consumers' satisfaction achievement," *Int. Trans. Electr. Energy Syst.*, vol. 29, no. 4, p. e2795, Apr. 2019, doi: 10.1002/etep.2795.

[3] A. M. Elsayed, M. M. Mishref, and S. M. Farrag, "Distribution system performance enhancement (Egyptian distribution system real case study)," *Int. Trans. Electr. Energy Syst.*, vol. 28, no. 6, p. e2545, Jun. 2018, doi: 10.1002/etep.2545.

[4] A. M. Shaheen, A. M. Elsayed, R. A. El-Sehiemy, and A. Y. Abdelaziz, "Equilibrium optimization algorithm for network reconfiguration and distributed generation allocation in power systems," *Appl. Soft Comput.*, vol. 98, Jan. 2021, Art. no. 106867, doi: 10.1016/j.asoc.2020.106867.

[5] E. Hooshmand and A. Rabiee, "Energy management in distribution systems, considering the impact of reconfiguration, RESs, ESSs and DR: A trade-off between cost and reliability," *Renew. Energy*, vol. 139, pp. 346–358, Aug. 2019, doi: 10.1016/j.renene.2019.02.101.

[6] F. Capitanescu, L. F. Ochoa, H. Margossian, and N. D. Hatziargyriou, "Assessing the potential of network reconfiguration to improve distributed generation hosting capacity in active distribution systems," *IEEE Trans. Power Syst.*, vol. 30, no. 1, pp. 346–356, Jan. 2015, doi: 10.1109/TPWRS.2014.2320895.

[7] C. Gerez, L. I. Silva, E. A. Belati, A. J. Sguarezi Filho, and E. C. M. Costa, "Distribution network reconfiguration using selective firefly algorithm and a load flow analysis criterion for reducing the search space," *IEEE Access*, vol. 7, pp. 67874–67888, 2019, doi: 10.1109/ACCESS.2019.2918480.

[8] A. Landeros, S. Koziel, and M. F. Abdel-Fattah, "Distribution network reconfiguration using feasibility-preserving evolutionary optimization," *J. Mod. Power Syst. Clean Energy*, vol. 7, no. 3, pp. 589–598, May 2019, doi: 10.1007/s40565-018-0480-7.

[9] S. Essallah, A. Khedher, and A. Bouallegue, "Integration of distributed generation in electrical grid: Optimal placement and sizing under different load conditions," *Comput. Electr. Eng.*, vol. 79, Oct. 2019, Art. no. 106461, doi: 10.1016/j.compeleceng.2019.106461.

[10] B. Owens, "The rise of distributed power," *Gen. Electr.*, vol. 47, 2014.

[11] M. A. Tolba, H. Rezk, M. Al-Dhaifallah, and A. A. Eisa, "Heuristic optimization techniques for connecting renewable distributed generators on distribution grids," *Neural Comput. Appl.*, vol. 32, no. 17, pp. 14195–14225, Sep. 2020, doi: 10.1007/s00521-020-04812-y.

[12] A. A. A. El-Ela, R. A. El-Sehiemy, A. M. Shaheen, and A. R. Ellien, "Optimal allocation of distributed generation units correlated with fault current limiter sites in distribution systems," *IEEE Syst. J.*, vol. 15, no. 2, pp. 2148–2155, Jun. 2021, doi: 10.1109/jsyst.2020.3009028.

[13] E. E. Elattar and S. K. Elsayed, "Optimal location and sizing of distributed generators based on renewable energy sources using modified moth flame optimization technique," *IEEE Access*, vol. 8, pp. 109625–109638, 2020, doi: 10.1109/ACCESS.2020.3001758.

[14] S. Kumar, K. K. Mandal, and N. Chakraborty, "Optimal DG placement by multi-objective opposition based chaotic differential evolution for techno-economic analysis," *Appl. Soft Comput.*, vol. 78, pp. 70–83, May 2019, doi: 10.1016/j.asoc.2019.02.013.

[15] A. A. A. El-Ela, S. M. Allam, A. M. Shaheen, and N. A. Nagem, "Optimal allocation of biomass distributed generation in distribution systems using equilibrium algorithm," *Int. Trans. Electr. Energy Syst.*, vol. 31, no. 2, Feb. 2021, doi: 10.1002/2050-7038.12727.

[16] A. M. Shaheen, E. E. Elattar, R. A. El-Sehiemy, and A. M. Elsayed, "An improved sunflower optimization algorithm-based Monte Carlo simulation for efficiency improvement of radial distribution systems considering wind power uncertainty," *IEEE Access*, vol. 9, pp. 2332–2344, 2021, doi: 10.1109/ACCESS.2020.3047671.

[17] K. Mahmoud and M. Lehtonen, "Simultaneous allocation of multi-type distributed generations and capacitors using generic analytical expressions," *IEEE Access*, vol. 7, pp. 182701–182710, 2019, doi: 10.1109/ACCESS.2019.2960152.

[18] K. Mahmoud and M. Lehtonen, "Three-level control strategy for minimizing voltage deviation and flicker in PV-rich distribution systems," *Int. J. Electr. Power Energy Syst.*, vol. 120, Sep. 2020, Art. no. 105997, doi: 10.1016/j.ijepes.2020.105997.

[19] M. Said, A. M. Shaheen, A. R. Ginidi, R. A. El-Sehiemy, K. Mahmoud, M. Lehtonen, and M. M. F. Darwish, "Estimating parameters of photovoltaic models using accurate turbulent flow of water optimizer," *Processes*, vol. 9, no. 4, p. 627, Apr. 2021, doi: 10.3390/pr9040627.

[20] M. A. S. Masoum, M. Ladjevardi, A. Jafarian, and E. F. Fuchs, "Optimal placement, replacement and sizing of capacitor banks in distorted distribution networks by genetic algorithms," *IEEE Trans. Power Del.*, vol. 19, no. 4, pp. 1794–1801, Oct. 2004, doi: 10.1109/TPWRD.2004.835438.

[21] K. Mahmoud and M. Lehtonen, "Direct approach for optimal allocation of multiple capacitors in distribution systems using novel analytical closed-form expressions," *Electr. Eng.*, vol. 103, no. 1, pp. 245–256, Feb. 2021, doi: 10.1007/s00202-020-01073-9.

[22] A. Selim, S. Kamel, and F. Jurado, "Capacitors allocation in distribution systems using a hybrid formulation based on analytical and two metaheuristic optimization techniques," *Comput. Electr. Eng.*, vol. 85, Jul. 2020, Art. no. 106675, doi: 10.1016/j.compeleceng.2020.106675.

[23] A. M. Shaheen and R. A. El-Sehiemy, "Enhanced feeder reconfiguration in primary distribution networks using backtracking search technique," *Aust. J. Electr. Electron. Eng.*, vol. 17, no. 13, pp. 196–202, Sep. 2020, doi: 10.1080/1448837X.2020.1817231.

[24] S. Kamel, A. Selim, F. Jurado, J. Yu, K. Xie, and T. Wu, "Capacitor allocation in distribution systems using fuzzy loss sensitivity factor with sine cosine algorithm," in *Proc. IEEE PES Innov. Smart Grid Technol. Asia (ISGT)*, May 2019, pp. 1276–1281, doi: 10.1109/ISGT-Asia.2019.8881794.

[25] F. H. Awad, A. A. Mansour, and E. E. A. Elzahab, "Thyristor controlled reactor with different topologies based on fuzzy logic controller," *Int. J. Eng. Res.*, vol. 4, no. 9, pp. 498–505, Sep. 2015, doi: 10.17950/ijer/v4s9/906.

[26] O. Arouna, M. I. Adolphe, A. O. Robert, A. Z. Kenneth, V. Antoine, B. Ramanou, T. Herman, and D. Celestin, "Technico-economic optimization of distributed generation (DG) and static var compensator (SVC) positioning in a real radial distribution network using the NSGA-II genetic algorithm," in *Proc. IEEE PES/IAS PowerAfrica*, Aug. 2019, pp. 42–47, doi: 10.1109/PowerAfrica.2019.8928631.

[27] R. Gitibin and F. Hoseinzadeh, "Comparison of D-SVC and D-STATCOM for performance enhancement of the distribution networks connected WECS including voltage dependent load models," in *Proc. 20th Conf. Electr. Power Distribution Netw. Conf. (EPDC)*, Apr. 2015, pp. 90–100, doi: 10.1109/EPDC.2015.7330479.

[28] R. Agrawal, S. Bharadwaj, S. K. Bharadwaj, and K. C. Muley, "Optimal location of static VAR compensator using evolutionary optimization techniques," *Int. J. Emerg. Technol.*, vol. 11, no. 1, pp. 245–256, 2020.

[29] D. Sen, S. R. Ghatak, and P. Acharjee, "Optimal allocation of static VAR compensator by a hybrid algorithm," *Energy Syst.*, vol. 10, no. 3, pp. 677–719, Aug. 2019, doi: 10.1007/s12667-017-0247-7.

[30] A. A. A. El-Ela, R. A. El-Sehiemy, A. M. Shaheen, and I. A. Eissa, "Optimal coordination of static VAR compensators, fixed capacitors, and distributed energy resources in Egyptian distribution networks," *Int. Trans. Electr. Energy Syst.*, vol. 30, no. 11, Nov. 2020, Art. no. e12609, doi: 10.1002/2050-7038.12609.

[31] C.-F. Chang, "Reconfiguration and capacitor placement for loss reduction of distribution systems by ant colony search algorithm," *IEEE Trans. Power Syst.*, vol. 23, no. 4, pp. 1747–1755, Nov. 2008, doi: 10.1109/TPWRS.2008.2002169.

[32] A. M. Shaheen, A. M. Elsayed, R. A. El-Sehiemy, S. Kamel, and S. S. M. Ghoneim, "A modified marine predators optimization algorithm for simultaneous network reconfiguration and distributed generator allocation in distribution systems under different loading conditions," *Eng. Optim.*, pp. 1–22, Apr. 2021, doi: 10.1080/0305215x.2021.1897799.

[33] T. T. Nguyen, T. T. Nguyen, N. A. Nguyen, and T. L. Duong, "A novel method based on coyote algorithm for simultaneous network reconfiguration and distribution generation placement," *AIN Shams Eng. J.*, vol. 12, no. 1, pp. 665–676, Mar. 2021, doi: 10.1016/j.asej.2020.06.005.

[34] R. Vempalle and P. K. Dhal, "Loss minimization by reconfiguration along with distributed generator placement at radial distribution system with hybrid optimization techniques," *Technol. Econ. Smart Grids Sustain. Energy*, vol. 5, no. 1, pp. 1–12, Dec. 2020, doi: 10.1007/s40866-020-00088-2.

[35] A. A. A. El-Ela, R. A. El-Sehiemy, and A. S. Abbas, "Optimal placement and sizing of distributed generation and capacitor banks in distribution systems using water cycle algorithm," *IEEE Syst. J.*, vol. 12, no. 4, pp. 3629–3636, Dec. 2018, doi: 10.1109/JSYST.2018.2796847.

[36] A. M. Shaheen and R. A. El-Sehiemy, "Optimal coordinated allocation of distributed generation units/capacitor banks/voltage regulators by EGWA," *IEEE Syst. J.*, vol. 15, no. 1, pp. 257–264, Mar. 2021, doi: 10.1109/jsyst.2020.2986647.

[37] K. Oikonomou, M. Parvania, and R. Khatami, "Deliverable energy flexibility scheduling for active distribution networks," *IEEE Trans. Smart Grid*, vol. 11, no. 1, pp. 655–664, Jan. 2020, doi: 10.1109/TSG.2019.2927604.

[38] Y. Li, B. Feng, G. Li, J. Qi, D. Zhao, and Y. Mu, "Optimal distributed generation planning in active distribution networks considering integration of energy storage," *Appl. Energy*, vol. 210, pp. 1073–1081, Jan. 2018, doi: 10.1016/j.apenergy.2017.08.008.

[39] T. Fetouh and A. M. Elsayed, "Optimal control and operation of fully automated distribution networks using improved tunicate swarm intelligent algorithm," *IEEE Access*, vol. 8, pp. 129689–129708, 2020, doi: 10.1109/ACCESS.2020.3009113.

[40] O. K. Siirto, A. Safdarian, M. Lehtonen, and M. Fotuhi-Firuzabad, "Optimal distribution network automation considering Earth fault events," *IEEE Trans. Smart Grid*, vol. 6, no. 2, pp. 1010–1018, Mar. 2015, doi: 10.1109/TSG.2014.2387471.

[41] M. McGranaghan and F. Goodman, "Technical and system requirements for advanced distribution automation," in *Proc. 18th Int. Conf. Exhib. Electr. Distrib. (CIRED)*, 2005, p. v5-93, doi: 10.1049/cp:20051374.

[42] J.-S. Chou and D.-N. Truong, "A novel metaheuristic optimizer inspired by behavior of jellyfish in ocean," *Appl. Math. Comput.*, vol. 389, Jan. 2021, Art. no. 125535, doi: 10.1016/j.amc.2020.125535.

[43] N. Mithulananthan, D. Q. Hung, and K. Y. Lee, "Intelligent network integration of distributed renewable generation," in *Green Energy and Technology*. Springer, 2017, doi: 10.1007/978-3-319-49271-1.

[44] A. M. Shaheen, R. A. El-Sehiemy, and S. M. Farrag, "A reactive power planning procedure considering iterative identification of VAR candidate buses," *Neural Comput. Appl.*, vol. 31, no. 3, pp. 653–674, Mar. 2019, doi: 10.1007/s00521-017-3098-1.

[45] A. M. Shaheen, S. R. Spea, S. M. Farrag, and M. A. Abido, "A review of meta-heuristic algorithms for reactive power planning problem," *Ain Shams Eng. J.*, vol. 9, no. 2, pp. 215–231, Jun. 2018, doi: 10.1016/j.asej.2015.12.003.

[46] A. M. Shaheen, R. A. El-Sehiemy, S. Kamel, E. E. Elattar, and A. M. Elsayed, "Improving distribution networks' consistency by optimal distribution system reconfiguration and distributed generations," *IEEE Access*, vol. 9, pp. 67186–67200, 2021.

[47] M. M. Aman, G. B. Jasmon, A. H. A. Bakar, and H. Mokhlis, "A new approach for optimum simultaneous multi-DG distributed generation units placement and sizing based on maximization of system loadability using HPSO (hybrid particle swarm optimization) algorithm," *Energy*, vol. 66, pp. 202–215, Mar. 2014, doi: 10.1016/j.energy.2013.12.037.

[48] A. A. A. El-Ela, A. M. Shaheen, R. A. El-Sehiemy, and N. K. El-Ayaa, "Optimal allocation of DGs with network reconfiguration using improved spotted hyena algorithm," *WSEAS Trans. Power Syst.*, vol. 15, pp. 60–67, Apr. 2020, doi: 10.37394/232016.2020.15.7.

[49] E. E. Elattar, A. M. Shaheen, A. M. El-Sayed, R. A. El-Sehiemy, and A. R. Ginidi, "Optimal operation of automated distribution networks based-MRFO algorithm," *IEEE Access*, vol. 9, pp. 19586–19601, 2021, doi: 10.1109/ACCESS.2021.3053479.

[50] A. M. Shaheen, A. R. Ginidi, R. A. El-Sehiemy, and E. E. Elattar, "Optimal economic power and heat dispatch in cogeneration systems including wind power," *Energy*, vol. 225, Jun. 2021, Art. no. 120263, doi: 10.1016/j.energy.2021.120263.

[51] E. A. Almabsout, R. A. El-Sehiemy, O. N. U. An, and O. Bayat, "A hybrid local search-genetic algorithm for simultaneous placement of DG units and shunt capacitors in radial distribution systems," *IEEE Access*, vol. 8, pp. 54465–54481, 2020, doi: 10.1109/ACCESS.2020.2981406.

[52] S. Kaur, L. K. Awasthi, A. L. Sangal, and G. Dhiman, "Tunicate swarm algorithm: A new bio-inspired based Metaheuristic paradigm for global optimization," *Eng. Appl. Artif. Intell.*, vol. 90, Apr. 2020, Art. no. 103541, doi: 10.1016/j.engappai.2020.103541.

[53] A. M. Shaheen, R. A. El-Sehiemy, E. E. Elattar, and A. S. Abd-Elrazek, "A modified crow search optimizer for solving non-linear OPF problem with emissions," *IEEE Access*, vol. 9, pp. 43107–43120, 2021, doi: 10.1109/ACCESS.2021.3060710.

[54] A. Shaheen, A. Elsayed, and R. El-Sehiemy, "Optimal economic–environmental operation for AC-MTDC grids by improved crow search algorithm," *IEEE Syst. J.*, early access, Jun. 8, 2021, doi: 10.1109/JSYST.2021.3076515.

[55] A. M. Shaheen, A. M. Elsayed, and R. A. El-Sehiemy, "Optimal distributed generation and capacitor placement in power distribution networks for power loss minimization," in *Proc. Int. Conf. Adv. Electr. Eng. (ICAEE)*, Jan. 2014, pp. 1–6, doi: 10.1109/ICAEE.2014.6838519.

[56] J. M. S. Pinheiro, C. R. R. Dornellas, M. T. Schilling, A. C. G. Melo, and J. C. O. Mello, "Probing the new IEEE reliability test system (RTS-96): HL-II assessment," *IEEE Trans. Power Syst.*, vol. 13, no. 1, pp. 171–176, Feb. 1998, doi: 10.1109/59.651632.